

CHEMICAL COMPOSITION AND SIZE DISTRIBUTIONS FOR FLY ASHES

Sarbajit Ghosal, Jon L. Ebert and Sidney A. Self

High Temperature Gasdynamics Laboratory,
Department of Mechanical Engineering,
Stanford University, Stanford, California.

Keywords: fly ash, composition distribution, size distribution.

1 INTRODUCTION

The aim of this paper is twofold: to present mathematical functions to describe and store CCSEM/AIA (Computer Controlled Scanning Electron Microscopy / Automatic Image Analysis) and size data for fly ashes, and to discuss two limitations of using single-particle measurement techniques to draw general conclusions about ash properties.

Fly ash characterization is complicated by the strong inter-particle variation in morphology, diameter and chemical composition. However, with the development of microanalytical tools such as CCSEM/AIA (e.g., Barta *et al*, 1990; Steadman *et al*, 1992), diameters and chemical compositions of individual particles for statistically significant sample sizes (>1000) can now be determined with relative ease.

It is necessary to store the large amounts of data generated by CCSEM analyses in convenient forms that can be easily manipulated. In this paper, simple mathematical functions are proposed which incorporate the information in differential and cumulative forms. The functions are used to detect size-composition correlations.

Ash size distribution was measured using the Coulter Multisizer. The broad size distribution of the ash is well described by the lognormal function truncated outside the measurement limits, and the detailed size information is stored compactly using four quantities.

It is observed that CCSEM may not present a complete picture of the distribution of oxides with significant size-composition correlation because of sampling limitations. This phenomenon is illustrated for iron oxide which is preferentially present in larger ash particles. Additionally, a comparison of the size distributions obtained with CCSEM, and with the Multisizer, shows that the former tends to overpredict the median size because of an artifact associated with sample preparation.

Measurements were made on ash samples from six representative coals collected in cyclones and baghouses of pilot and full-scale power plants. These coals are Illinois #6, Kentucky #9, Upper Freeport, PA, (all three bituminous), Beulah, ND, and San Miguel, TX (both lignites), and Eagle Butte, WY (sub-bituminous). The San Miguel and the Eagle Butte ashes were obtained from full-scale power plants. The other four ashes were generated at the pilot-scale facilities of Foster Wheeler, and collected using a cyclone and baghouse in sequence. However, for these four, the whole ashes could not be reconstituted due to unavailability of information on the relative proportions of baghouse and cyclone ashes. They were characterized separately with respect to their chemical, density, and size distributions. Due to space limitations, in general only one or two ashes are cited here as examples. Complete analyses for all six ashes (including a description of sample preparation techniques for CCSEM analysis) are presented by Ghosal (1993).

2 COMPOSITION DISTRIBUTION FUNCTIONS

For all six ashes, 1000–1800 particles were selected at random by the CCSEM software. Their diameters were measured and their compositions analyzed with respect to the following twelve elements: Si, Al, Fe, Ca, Mg, Na, K, Ti, Ba, S, P, and Cl. For such sample sizes, the numbers of particles detected per micron-bin drop sharply and steadily for diameters $\geq 5 \mu\text{m}$. In general, it was seen that particles with diameter $< 8 \mu\text{m}$ constitute $\geq 90\%$ of the sample. However, the larger diameter bins contain insufficient numbers of particles, and should not be considered for drawing conclusions on size-composition relationships. A minimum population of twenty-five particles per micron-bin was arbitrarily chosen to determine the upper diameter limit, D_{25} .

Ash samples (40–50 g each) were melted and quenched rapidly to form glassy slags. Polished samples were prepared for chemical composition analysis using electron microprobe. Appropriate detectors and standards were used to measure the concentrations of the above twelve elements. Because each slag is prepared from a large ash sample, the analysis accurately yields the bulk (average) composition of the ash. The elemental compositions from both CCSEM and microprobe data were converted to oxide compositions using the following formulae: SiO_2 , Al_2O_3 , Fe_2O_3 , CaO , MgO , Na_2O , K_2O , TiO_2 , BaO , SO_3 , and P_2O_5 .

The mineral matter in coal is present in equilibrium, crystalline phases, generally having fixed compositions. However, the composition distribution of the ash particles is much more continuous. This is a result of the complex formation process, whereby the mineral inclusions melt, coalesce, and cool rapidly to form (primarily) spherical glassy ash particles. Hence, it is appropriate to use mathematical functions to describe inter-particle compositional variation. The following functions are proposed to describe the composition distribution for a single ash particle, and also to determine size-composition relationships.

1. The function, $c_o(D)$, is defined so that $c_o(D) dD$ represents the mass fraction (or %) of oxide o present in particles with diameters between D and $D + dD$. Integrating $c_o(D)$ over all diameters yields the average mass fraction of oxide o in the ash.
2. The second function $\xi_o(x, D)$ is defined so that $\xi_o(x, D) dx dD$ represents the volume fraction of ash with mass fraction of oxide o between x and $x + dx$ made up of particles with diameters between D and $D + dD$.
3. Finally, there is a function, $\zeta_o(x)$, such that $\zeta_o(x) dx$ represents the number fraction of ash particles with mass percentage of oxide o between x and $x + dx$.

A convenient way to study size-composition relationships is to use a cumulative function, $C_o(D)$, defined as

$$C_o(D) = \frac{\int_0^D c_o(x) x^3 dx}{\int_0^D x^3 dx}$$

Thus, $C_o(D)$ is the average mass fraction of oxide o for all ash particles with diameters less than D . Figure 1 shows the distribution $C_o(D_{25})$ for the Illinois and Beulah ashes. The cumulative number distribution, $F_o(D)$, shows the fraction of the sample included in calculating $C_o(D)$. The magnitude of the slope of $C_o(D)$ indicates the magnitude of size-composition correlation.

Among all six ashes, it is noted that only two, Illinois #6 and Kentucky #9 (not shown here), have an average Fe_2O_3 content $> 5\%$. While the iron content showed a small decrease with increasing diameter for the Illinois and Kentucky ashes over the whole size range, it showed no dependence on size for the other four. Similarly, CaO showed a very small decrease with increasing diameter for some of the ashes. In general, the $C_{Al}(D)$, $C_{Fe}(D)$, and $C_{Ca}(D)$ graphs are flat, indicating that there is negligible correlation between particle size and composition.

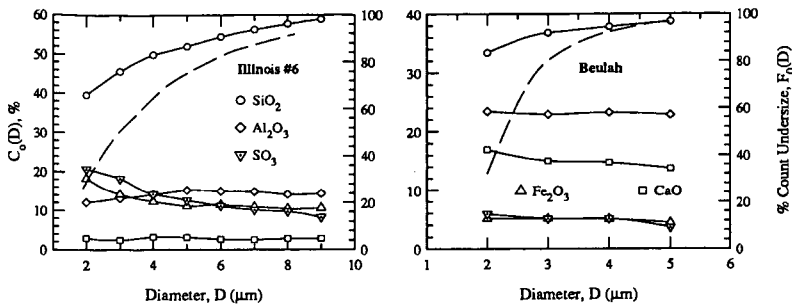


Figure 1: Cumulative undersize composition distribution. The right hand axis shows the count undersize, which is graphed as a dashed line.

Consistent size-composition trends are shown by sulfur and silica. The sulfates are deposited preferentially on smaller particles which confirms earlier reports (e.g., Ramsden and Shibaoka, 1982). However, the size-dependence of SO_3 is strong in some ashes (e.g., Illinois #6) and weak in others (e.g., Beulah). The positive size-concentration relationship for SiO_2 is noted in five of the six ashes, with the exception of the atypical calcia- and alumina-rich Eagle Butte ash. As discussed later, many of the large ash particles ($D \geq 10 \mu m$), not detected here, are relatively iron-rich. Hence, the slope of $C_{Fe}(D)$ can be expected to increase significantly at larger diameters. Similar observations with respect to size and composition relationships for the major oxides are reported by Mamane *et al* (1986) who studied Al/Si distribution as a function of particle diameter, and Hemmings and Berry (1986) who analysed the average composition of size-classified ash derived from sub-bituminous coal.

The distribution of the oxides in the ash volume can be expressed on a cumulative basis by integrating $\xi_o(x, D)$ in the following manner

$$f_o(x) = \int_0^x \int_0^{D_{25}} \xi_o(x', D) dD dz'$$

Here, $f_o(x)$ is the volume fraction of ash with mass percent of oxide o less than x . Particles with $D > D_{25}$ are omitted. When $x=100\%$, $f_o(x)$ is unity for each of the oxides. Figure 2 presents $f_o(x)$ for the Illinois and Beulah ashes, and its interpretation gives some useful information. Large or small slopes over an increment of Δx implies the presence of a large or small proportion of particles with oxide content between x and $x + \Delta x$, respectively. Among all oxides, silica is distributed most broadly (i.e., with the largest range of mass fractions), with Illinois ash having the broadest $f_o(x)$.

Both Kentucky and Illinois ashes are found to contain a significant volume fraction of silica-rich particles (i.e., $>80\%$ SiO_2). Although Al_2O_3 is one of the two most predominant oxides, there are no alumina-rich particles (i.e., $\geq 60\%$). For iron, it is seen that 90% of the ash volume contains $\leq 8\%$ of iron (by mass) for all the ashes, with the exception of Illinois #6 (which has a broader distribution with only 65% of the ash volume containing $<8\%$ of Fe_2O_3). Hence, for all ashes except Illinois #6, the fraction of ash volume containing a wide range of Fe_2O_3 mass fraction (20%-50%) is negligible. The distribution of CaO is similar to that of Fe_2O_3 in most of the ashes, except in Eagle Butte ash (not shown here) where it is the main constituent, and resembles the Al_2O_3 distribution of the other ashes. The four oxides shown are clearly the major constituents since, for all ashes, only 10% of the ash volume is seen to contain more than 10% of the other oxides by mass.

Representation of ash composition as cumulative distribution functions, as presented in Figure 2, represents significant reduction of the overall data size. For example, for twelve oxides, one could tabulate

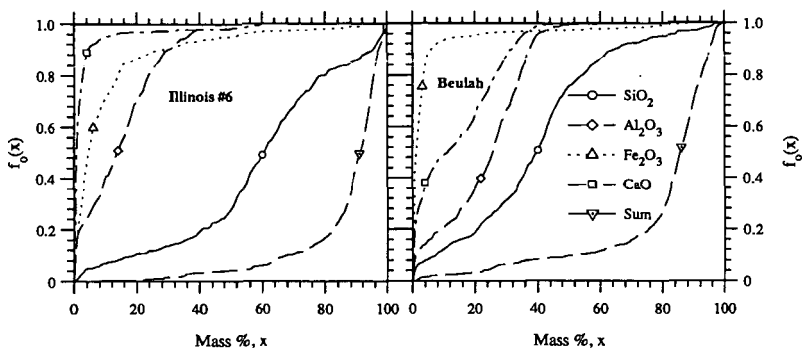


Figure 2: Volume-composition distribution shown on a cumulative basis. $f_o(x)$ represents the volume of ash with mass fraction of oxide o less than $x\%$, as a fraction of the total volume.

$f_o(x)$ at 1% intervals for a total of 1200 stored values (many of which are zero since many of the minor oxides occur in only trace amounts). Alternatively, these distribution functions may be fitted with appropriate polynomials if additional data compression is desired.

The primary limitation of this scheme is that it does not allow for correlation between the various species, or with particle size. As illustrated in Figure 1, the correlation between composition and size is not significant for the ashes studied here. Analysis of the linear correlation coefficient, R , for the twelve oxides revealed that there are generally no significant correlations between any two oxides, although BaO and TiO₂ were exceptions with $R \approx 0.7$ for the Illinois #6 ash.

3 IRON DISTRIBUTION IN ASHES

An average ash composition, ϑ_o , was obtained by combining the CCSEM data with the volume distribution, $F_3(D)$, obtained from the Multisizer data (Ghosal, 1993). For all ashes, it was found that $1\% < \vartheta_{Fe} < 13\%$ (Table 1), which is only 25%–70% of that determined by microprobe analysis. The reason for this discrepancy appears to be statistical. Size measurements of the iron-rich ash fractions, separated into classes by centrifugal separation (Ghosal, 1993), show that they have significantly higher median diameters than that of the whole (unseparated) ash. Consequently, they are fewer in number, and a typical CCSEM sample size of one or two thousand particles is not statistically large enough to detect sufficient numbers of such particles, in contrast to the microprobe data which is averaged over a large sample.

It is noted that a large CCSEM sample is needed for an accurate estimate of the average iron content even if iron distribution is not weighted in favor of larger particles because Fe₂O₃ constitutes <20% or less of the ash mass. Simple statistical analyses suggest that a sample size of >15,000 particles is needed for estimating the *bulk* iron content of the Kentucky ash with a confidence interval of 0.5% (Ghosal, 1993). Nevertheless, CCSEM analyses provides useful information about iron distribution among the smaller ash particles ($D \lesssim 7 \mu\text{m}$).

Table 1: Average Fe₂O₃ content of ashes (by mass) obtained from CCSEM and electron microprobe analyses illustrating the underprediction of the iron content from CCSEM data.

Fly Ash	CCSEM, ϑ_o	Microprobe	Ratio, ϑ_o /Microprobe
Kentucky #9	6.9%	12.59%	0.55
Illinois #6	13.0%	18.96%	0.69
Upper Freeport	4.8%	13.05%	0.37
Eagle Butte	3.1%	6.88%	0.45
Beulah	4.6%	16.88%	0.27
San Miguel	1.2%	2.75%	0.44

4 ASH SIZE DISTRIBUTION

Fly ash has a broad size distribution with diameters spanning more than three orders of magnitude. Hence, it is important to measure the dispersion of the size distribution (i.e., the standard deviation). In the few references giving size data (e.g., Fisher, *et al*, 1978; Wall, *et al*, 1981; Hemmings and Berry, 1986), only median diameters are discussed. Furthermore, a suitable mathematical function is needed to describe the size distribution. Such a function allows for comparison of various ashes, and are also needed for computation of properties of ash aerosols, e.g., radiative properties (Ghosal and Self, 1993).

A method for accurate measurement of ash size distribution (for particle diameters $\gtrsim 1 \mu\text{m}$) using the Coulter Multisizer is presented by Ghosal *et al* (1993). For powders (such as fly ash) with size distributions that are typically very broad and skewed toward small particles, lognormal functions are commonly used to describe the size distributions (Crow and Shimizu, 1988). However, because of lack of size information outside the measurement limits set by the dynamic range of the Multisizer, the data are fitted to a function truncated outside the measurement limits (a, b). The form of this truncated lognormal distribution function, characterized by a number median diameter, D_n , and a geometric standard deviation (GSD), σ_g , is shown below:

$$\frac{dF^{(a,b)}(D)}{d(\ln D)} = \frac{\frac{1}{(2\pi)^{1/2} \ln \sigma_g} \exp \left[-\frac{1}{2} \left(\frac{\ln D/D_n}{\ln \sigma_g} \right)^2 \right]}{\int_{\ln a}^{\ln b} \frac{1}{(2\pi)^{1/2} \ln \sigma_g} \exp \left[-\frac{1}{2} \left(\frac{\ln x/D_n}{\ln \sigma_g} \right)^2 \right] d(\ln x)} \quad a \leq D \leq b$$

The surface area and volume distributions are the second and third moments, respectively, of the above number (or count) distribution. All have the same value of σ_g . Thus, if one median diameter and σ_g are known, the other two can be calculated (Crow and Shimizu, 1988). In this manner, detailed information on the ash size distribution can be stored compactly using four quantities: D_v , σ_g , a , and b . For example, for the Upper Freeport as 1, these numbers are $9.3 \mu\text{m}$, 2.76 , $1.2 \mu\text{m}$, and $60 \mu\text{m}$, respectively. The median diameters by number count and area are respectively $D_n=0.4 \mu\text{m}$ and $D_a=3.3 \mu\text{m}$.

The above function was found to fit the size data very well, and the best-fit values of median diameters and GSD are shown in Table 2. The values of D_v and σ_g tend to fall in the ranges of 9–15 μm and 2.0–3.0, respectively with one exception. The San Miguel lignite ash, which is highly cenospheric, contains many large particles, and its D_v is two to three times larger than that of the other ashes. For many of the ashes, the values of D_n are below the lower limit of measurement, and the number of particles detected in each Multisizer size channel continues to increase with decreasing diameter. Best-fit parameters calculated for the data of Wall *et al* (1981) were found to be $D_v=10.5 \mu\text{m}$ and $\sigma_g=2.95$, within the ranges observed in this study.

Table 2: Size parameters for best-fit lognormal functions used to represent the size distributions of the fly ashes studied. The truncation limits, (a, b) , are $(1.2 \mu\text{m}, 180.0 \mu\text{m})$ for the San Miguel ash, and $(1.2 \mu\text{m}, 60.0 \mu\text{m})$ for the remaining ashes.

Fly ash	Coal Type	Collection	D_n	D_a	D_v	D_{32}	σ_g
Kentucky #9	Bituminous	Baghouse	1.2	5.1	10.4	7.3	2.33
Kentucky #9	Bituminous	Cyclone	3.4	9.4	15.6	12.1	2.04
Illinois #6	Bituminous	Baghouse	0.4	3.4	10.1	5.8	2.85
Illinois #6	Bituminous	Cyclone	2.3	7.9	14.6	10.7	2.19
Beulah, ND	Lignite	Baghouse	0.4	3.9	12.7	7.0	2.98
Beulah, ND	Lignite	Cyclone	1.2	5.4	11.5	7.9	2.39
Upper Freeport, PA	Bituminous	Baghouse	0.4	3.3	9.3	5.6	2.76
San Miguel, TX	Lignite	ESP	1.1	10.5	32.3	18.4	2.89
Eagle Butte, WY	Sub-bituminous	Baghouse	0.6	5.0	14.3	8.4	2.80

4.1 Comparison of CCSEM Size Distribution with Multisizer Data

The geometric diameters of ash particles are determined using an image analyzing program that computes the average length of eight 'chords' passing through the 'center' of the particle as determined by an appropriate algorithm. Size distributions were computed from this data. The cumulative undersize form of the lognormal distribution plots as a straight line on a log-probability graph. However, for the truncated function, there is a departure from the straight line at the large and small diameter limits. The volume distribution obtained from the CCSEM data is plotted along with the Multisizer distribution for the Kentucky #9 ash in Figure 3.

It is virtually impossible to prepare a fully deagglomerated ash sample for CCSEM. The freeze-drying method used here (Ghosal, 1993) produces well-deagglomerated samples with very few particle clusters per SEM frame (which were rejected by limiting the acceptable range of shape factors). However, these few ash particle clusters typically consist of numerous small ash particles ($1-5 \mu\text{m}$) attached to one or two larger particles. Consequently, there is a deficit of small fly ash particles among those analyzed by CCSEM. The Multisizer data shows that D_v from CCSEM data is about 40% larger than that of the Multisizer distribution. No study of the effect of sample preparation on CCSEM size distribution could be located in the literature.

The difference in the two distributions in the large diameter ranges is due to statistical reasons. Because of the much larger sample size, the large ash particles are better represented in the Multisizer sample ($>150,000$ particles) than in the CCSEM sample (≈ 1000 particles). The Multisizer sampled 23 particles of diameter $>50 \mu\text{m}$. Using this data, it is seen that a random CCSEM sample size of ≈ 4000 particles is necessary to encounter one particle of diameter $>50 \mu\text{m}$. Additionally, it is possible that some of these 'rare' large particles are rejected as part of agglomerates.

These artifacts explain the departure of the CCSEM curve from the Multisizer curve in the smaller and larger diameter ranges, respectively. While the median diameter from SEM data depends on which of the factors predominates², the standard deviation is necessarily smaller because the range of particles examined is narrower. Hence, the slope of the size distribution is slightly steeper compared to the Multisizer distribution for each ash (Figure 3). These observations illustrate the limitations of measuring size distributions of powders with a broad size range using microscopes. It may account for discrepancies between ash size distributions measured using SEM and Coulter Counter reported by Fisher *et al* (1978),

²For the Kentucky #9 ash, the effect of the shortage of small particles predominates.

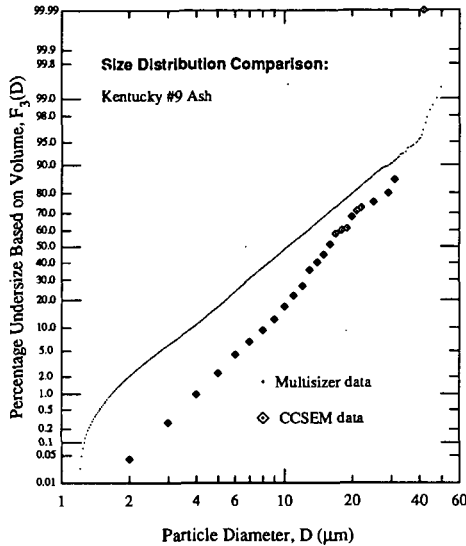


Figure 3: Comparison of Kentucky #9 ash size distribution obtained with Coulter Multisizer measurements (combining data obtained using 30 μm and 100 μm orifices) with CCSEM size data.

between ash size distributions measured using SEM and Coulter Counter reported by Fisher *et al* (1978), but not explained.

5 SUMMARY AND CONCLUSIONS

Although chemical composition measurement on a particle-by-particle basis using CCSEM confirmed significant inter-particle variation, correlation between size and composition is seen only for SiO_2 , and SO_3 . This observation is valid for ash particles with $D \lesssim 8 \mu\text{m}$, which comprise over 90% by number, and $\approx 50\%$ by volume, of the ashes in general. From this and other studies (see Ghosal, 1993), it was found that a large fraction of the iron is concentrated in relatively few, large particles. Thus, to get comprehensive and statistically reliable data using currently feasible CCSEM sample sizes, it appears necessary to perform CCSEM on accurately size-classified ashes.

Mathematical functions were used to describe oxide distributions in the ash. Cumulative distribution functions provide a means of representing the large volume of CCSEM data in a more compact form. The loss of oxide-to-oxide composition correlation associated with this representation is not important for many applications, such as characterization of the optical properties of fly ash.

Accurate size measurements made with the Coulter Multisizer showed that a truncated lognormal function describes the ash size distribution quite well. The differences between the size distributions obtained using the Multisizer and CCSEM are explained in terms of artifacts related to the SEM sample preparation technique, and statistical limitations imposed by sample size.

Acknowledgements: This work was supported by DOE under contract number DE-AC22-87PC 79903. The CCSEM measurements were made at the Energy and Environment Research Center of Grand Forks, ND.

References

- [1] Barta, L. E., *et al*, 1990, "A Statistical Investigation on Particle to Particle Variation of Fly Ash Using SEM-AIA-EDAX Technique", *Material Research Society Symposium Proceedings*, Vol. 178, pp. 67-82.
- [2] Crow, E. L., and Shimizu, K., 1988, *Lognormal Distributions*, Marcel Dekker Inc., New York.
- [3] Fisher, G. L., *et al*, 1978, "Physical and Morphological Studies of Size-Classified Coal Fly Ash", *Environmental Science and Technology*, Vol. 12, No. 4, pp. 447-451.
- [4] Ghosal, S. (1993), "Optical Characterization of Coal Fly Ashes and Infrared Extinction Measurements on Ash Suspensions", Ph. D. thesis, Mechanical Engineering Department, Stanford University, Stanford, CA 94305.
- [5] Ghosal, S., and Self, S. A., 1993, "Optical Characterization of Coal Fly Ash", presented at the 29th ASME/AIChE National Heat Transfer Conference, Atlanta.
- [6] Ghosal, S., Ebert, J. L., and Self, S. A., 1993, "Fly Ash Size Distributions: Use of Coulter Multisizer and Fitting to Truncated Lognormal Distributions", *Particle and Particle Systems Characterization*, Vol. 10, pp. 11-18.
- [7] Hemmings, R. T., and Berry, E. E., 1986, "Speciation in Size and Density Fractionated Fly Ash", *Material Research Society Symposium Proceedings*, Vol. 65, pp. 91-104.
- [8] Mamane, Y., Miller, J. L., and Dzubay, T. G., 1986, "Characterization of Individual Fly Ash Particles Emitted from Coa. and Oil-Fired Power Plants", *Atmospheric Environment*, Vol. 20, No. 11, pp. 2125-2135.
- [9] Ramsden, A. R., and Shibaoka, M., 1982, "Characterization and Analysis of Individual Fly Ash Particles from Coal-fired Power Stations by a Combination of Optical Microscopy, Electron Microscopy and Quantitative Electron Microprobe Analysis", *Atmospheric Environment*, Vol. 16, No. 9, pp. 2191-2206.
- [10] Steadman, E. N., *et al*, 1992, "Coal and Ash Characterization: Digital Image Analysis Applications", in *Inorganic Transformation and Ash Deposition During Combustion*, Ed: S. A. Benson, ASME, New York.
- [11] Wall, T. F., *et al*, 1981, "Fly Ash Characteristics and Radiative Heat Transfer in Pulverized-Coal-Fired Furnaces", *Combustion Science and Technology*, Vol. 26, pp. 107-121.